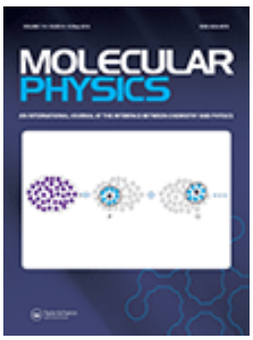

Taylor & Francis
Taylor & Francis Group

Molecular Physics

An International Journal at the Interface Between Chemistry and Physics

ISSN: 0026-8976 (Print) 1362-3028 (Online) Journal homepage: https://www.tandfonline.com/loi/tmph20

Superatomic properties of transition-metal-doped tetrahexahedral lithium clusters: TM@Li_{14}

Lijuan Yan, Jun Liu & Jianmei Shao

To cite this article: Lijuan Yan, Jun Liu & Jianmei Shao (2019): Superatomic properties of transition-metal-doped tetrahexahedral lithium clusters: TM@Li_{14}, Molecular Physics, DOI: 10.1080/00268976.2019.1592256

To link to this article: https://doi.org/10.1080/00268976.2019.1592256

Published online: 18 Mar 2019.

Submit your article to this journal

Article views: 207

View related articles

View Crossmark data

Citing articles: 1 View citing articles

Full Terms & Conditions of access and use can be found at
https://www.tandfonline.com/action/journalInformation?journalCode=tmph20

MOLECULAR PHYSICS
https://doi.org/10.1080/00268976.2019.1592256

Taylor & Francis
Taylor & Francis Group

RESEARCH ARTICLE

Check for updates

Superatomic properties of transition-metal-doped tetrahexahedral lithium clusters: TM@Li_{14}

Lijuan Yan[a], Jun Liu[b] and Jianmei Shao[a]

[a]College of Electronics & Information Engineering, Guangdong Ocean University, Zhanjiang, People's Republic of China; [b]College of Physics Science and Technology, Guangxi Normal University, Guilin, People's Republic of China

ABSTRACT

The lowest energy structure of Li_{15} cluster is a capped double centred square antiprism sharing a square face. Interestingly, when a lithium atom is substituted by a transition-metal atom TM (TM = Sc, Ti, V, Y, Zr, Nb, Hf, Ta and W), the lowest energy structure is found to be cage-like with a D_{6d} symmetry, where the outer cage is composed by fourteen lithium atoms with an endohedral transition-metal atom. The unique structures are confirmed by CALYSPO structure prediction method code and density-functional theory calculations. Superatomic properties are confirmed in all the D_{6d} clusters. Energy calculations predict that they are very stable, and their stability is further enhanced by the large gaps of the highest occupied molecular orbital and the lowest unoccupied molecular orbital (HOMO–LUMO gaps). Our findings offer potential applications in building blocks for assembling materials with superatoms.

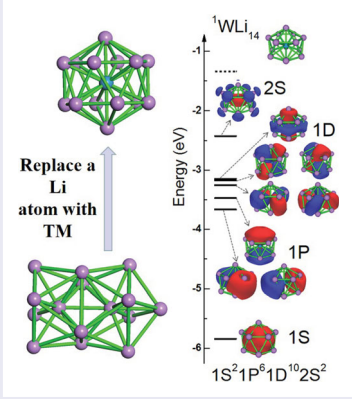

ARTICLE HISTORY
Received 3 November 2018
Accepted 4 March 2019

KEYWORDS
The jellium model; superatoms; transition-metal doped; magnetic moment; energy gap

Introduction

One of the important directions in the field of nanoscale science is developed to design stable clusters with specific features, which can be used as the primary building blocks to assemble functional materials, for the properties of clusters are strongly dependent with their sizes, shapes, compositions and the charged states [1–5]. In some case, the high stability of clusters with the chemical behaviour are analogous to individual elements, and the electronic states in these clusters are grouped into electronic shells similar to the situation of atoms. Such clusters can be viewed as superatoms [6]. For example, the 40 valence electrons of icosahedral Al_{13}^- cluster with a centred aluminium is known for its pronounced stability, and it can mimic the properties of a chloride ion [7]. Researching shows that such high stability of the Al_{13}^- cluster origins from just closures of geometric and electronic shells.

However, the electronic arrangement of superatomic orbitals is generally different from the Hund's rule, where the filling of a single atom orbital follows. Assembled by atoms, superatoms could undergo with spatial distortions to produce lower energy states for the occupation of paired electrons, which counteracts the Hund's coupling of maximum spin multiplicity. For metal clusters, their stability can be successfully understood according

CONTACT Lijuan Yan ylj_gdou@126.com; Jianmei Shao shaojm89@163.com

© 2019 Informa UK Limited, trading as Taylor & Francis Group

to the jellium model that the ionic charge of the cluster's atomic nuclei and the innermost electrons are regarded as a uniform positive spherical background, and the movement of valence electrons are subjected to an external potential [8–10]. Therefore, the filling of electronic levels for these metal clusters can be labelled as $1S^2|1P^6|1D^{10}|2S^21F^{14}|2P^61G^{18}|2D^{10}3S^{21}H^{22}|\ldots$, where S, P, D, F, G, H, are used to characterise superorbitals in superatoms, and the associated with magic numbers of the superatom are 2, 8, 18, 20, 34, 40, 58, 68, 90, etc. According to the model, the corresponding electronic configuration of Al_{13}^- cluster is $1S^21P^61D^{10}2S^21F^{14}2P^6$. All of electrons are paired and the closed electronic shell further enhances its stability resulting it remarkably stable.

Of course, some clusters with unpaired electrons can be still stable. Khanna and collaborators first reported two typical examples of an isolated VCs_8 cluster and a ligated $MnAu_{24}(SH)_{18}$ cluster, both with the maximum magnetic moment of 5 μ_B for a half-filled d subshell, respectively. Thereby, these clusters were regarded as magnetic superatoms. Moreover, a composite system was proposed to design magnetic superatoms in theoretical approach, where some atoms of the system had relatively localised orbitals providing the magnetic moment, and others with diffuse valence orbitals imparted the stability of the whole system [11]. This project opened a new research direction to design stable clusters and new superatoms though infusing transition-metal atoms in clusters. Since then, many magnetic superatoms have been developed [12–18].

In the paper, we are starting with lithium clusters for lithium atom is the lightest metal with a simple electronic shell of $1s^22s^1$, which is an ideal prototype to discuss the properties of simple metal clusters. However, the recent research advances of pure lithium clusters are relative scarcity, and most research interest is concentrating on lithium materials for their high power and capacity in energy storage devices, such as lithium ion batteries [19,20], hydrogen storage [21,22], and so on. Noteworthy, taking lithium clusters as an example, Cheng and Yang proposed a new concept of super valence bond (SVB) in 2013 year, of which superatoms can share both valence pairs and nuclei for shell closure thus forming delocalised super bonding [23]. Based on the SVB model, many stability of nonspherical metal clusters can give a reasonable interpretation [23–27]. Moreover, an amount of researches on doping lithium clusters with an impurity atom have been carried out as a result that the properties of lithium clusters change significantly [14,28–30].

Considering this, we replace a lithium atom of the pure lithium Li_{15} cluster with a transition-metal atom TM (TM = Sc, Ti, V, Y, Zr, Nb, Hf, Ta and W), and find that all the lowest energy structures of $TM@Li_{14}$ (TM = Sc, Ti, V, Y, Zr, Nb, Hf, Ta and W) clusters are a D_{6d} symmetry cage with the transition-metal atom embedded in the centre of the cage. Their stability is analysed from the aspects of geometric structures, electronic properties, magnetic properties, energy calculations and HOMO–LUMO gaps in this work.

Computational method

The search of the low energy structures of $TM@Li_{14}$ (TM = Sc, Ti, V, Y, Zr, Nb, Hf, Ta and W) clusters are using CALYSPO (Crystal structure AnaLYsis by Particle Swarm Optimization) code [31], which is an efficient structure prediction method, based on globally minimising potential energy surfaces evaluated by ab initio density-functional theory (DFT) calculations. Then, the acquired lowest energy structures are re-optimised at the DFT level by adopting the Perdew and Wang's 1991 exchange and gradient-corrected correlation functional (PW91) within the generalised gradient approximation (GGA) [32], the 1996 functional of Perdew, Burke and Ernzerhof (PBE) [33] as the studies of VLi_n (n = 1–13) clusters [29]. Considering the progress of DFT [34] and the assessment of density functionals for transition-metal compounds [35–37], other functionals are also studied for comparison. These include meta-GGA functional M06-L [38] and hybrid functional TPSSH [39], which is an abbreviation of the corresponding pure functional combining 10% of exact exchange. The calculations of harmonic vibrational frequencies prove that these lowest energy isomers are a true energy minimum because there is no imaginary frequency for all the lowest energy structures shown here. Furthermore, a series of spin multiplicities (SMs) are also considered to search for the electronic configurations with energy minimum for each optimised lowest energy structures. For MO analysis, a small basis set LANL2MB for all the atoms is applied as it produces a small variation of MO [40]. Relatively large basis set SDD is used to describe the transition-metal atoms and the lithium atoms for energy calculations [41]. All the DFT calculations are completed on Gaussian 16 package [42], and molecular visualisation is performed using Multiwfn_3.6 [43].

Results and discussion

As a starting point of discussion, the low energy structures of $W@Li_{14}$ cluster and the corresponding bare Li_{15} cluster are systematically studied by using the unbiased CALYPSO structure prediction method code. A large number of stable isomers are obtained, where the eight low energy isomers of $W@Li_{14}$ cluster are shown in

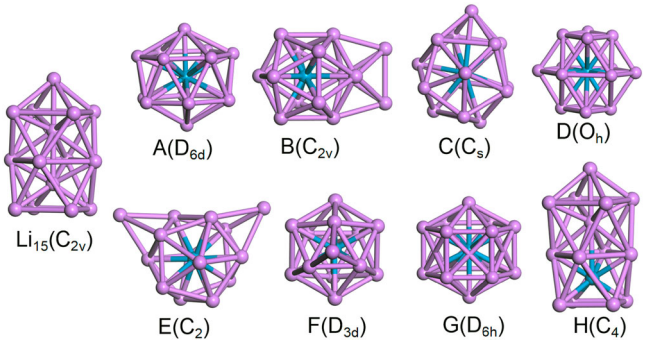

Figure 1. The lowest-energy structures and the eight low-lying isomers of TM@Li_{14} (TM = Sc, Ti, V and W) are shown. The cyan atom is transition-metal atoms (Sc, Ti, V and W); others are lithium. The lowest-energy structure of pure Li_{15} cluster is also displayed.

Figure 1, and the relative energies of these isomers are listed in Table 1. As previously reported in the literature [28], the lowest energy structure of pure Li_{15} cluster is a double centred square antiprism capped with a top lithium atom, and the two antiprisms share a square face. However, when a lithium atom is replaced with a tungsten atom, the structures completely change on the basis of our researches. The lowest energy structure of W@Li_{14} cluster is found to be like a cage with D_{6d} symmetry, where the fourteen lithium atoms are an arrangement to an outer shell cage and the tungsten atom is embedded in the centre of the cage. Inspired by the result of replacement one lithium atom with a tungsten atom to yield the lowest energy isomers with high symmetry, we further extend all the 3d transition-metal elements as the dopants to replace a lithium atom of the pure Li_{15} cluster. For the Sc, Ti, V atoms doped systems, their lowest energy isomers are still the D_{6d} symmetry cage with the centre decorated by a transition-metal atom, while for Cr, Mn, Fe, Co, Ni, Cu and Zn atoms as dopants, the D_{6d} symmetry cage isomers are not the lowest energy as shown in Table 1. Moreover, using the elements in the same main group as dopants the lowest energy isomers are similar, for instance, doped with Y, Zr, Hf, Nb and Ta atoms, where their lowest energy isomers are all the D_{6d} symmetry cage resemblance to the situation of Sc, Ti and V atoms as dopants, respectively. To simplify the discussion, in the following sections, TM@Li_{14} (TM = Sc, Ti, V and W) are chosen as representative clusters, and the properties of the same main group as dopants can be analogised except Cr, Mo and W atoms due to their difference of lowest energy isomers.

The stability of clusters is mainly determined by the closed geometric shells and electronic shells. Obviously, the caged TM@Li_{14} (TM = Sc, Ti, V and W) clusters have a closed geometric shell. Based on the jellium model, their electronic shells are analysed. In the W@Li_{14} cluster, the effective valence electrons are $2s^1$ for lithium atoms and $5d^46s^2$ for tungsten atom, where other electrons are mainly localised as lone pairs (LPs). Therefore, the total effective valence electrons are $n+6$, and the relevant number of effective valence electrons is 20 for W@Li_{14} cluster. Figure 2 shows the corresponding one electron energy levels and molecular orbitals (MOs). The lowest state has a 1S character which is spread over the whole cluster. The next three states have $1P_x$, $1P_y$ and $1P_z$ characteristics, where the degeneracy of the 1P orbitals is broken because of the oblate shape of the cluster leading to $1P_z$ non-degenerate about 0.23 eV higher in energy than the $1P_x$, $1P_y$ states under PW91/SDD level. By the same reason, the next five 1D orbitals have been broken into three groups of 2, 2 and 1 orbitals due to a crystal field splitting. The last state has a 2S character for the features of the MO diffuse over the entire cluster. Thus,

Table 1. Relative energies of TM@Li_{14} (TM = Sc, Ti, V, Cr, Mn, Fe, Co, Ni, Cu, Zn, Y, Zr, Nb, Mo, Hf, Ta and W) clusters, where the energies of their own lowest-energy isomers are chosen as references with 0.00 eV.

TM	A	B	C	D	E	F	G	H
Sc	0	0.26	0.35	0.51	A	A	0.60	1.60
Y	0	0.24	0.31	0.49	A	A	0.52	1.72
Ti	0	A	0.30	0.43	A	0.40	0.53	2.07
Zr	0	0.26	0.27	0.39	A	0.38	0.49	1.86
Hf	0	A	0.27	0.38	A	0.39	0.50	1.77
V	0	0.12	0.20	0.36	0.45	0.50	0.49	1.14
Nb	0	0.43	0.28	0.40	0.76	0.76	0.50	1.30
Ta	0	0.27	0.27	0.35	A	0.34	0.49	3.17
Cr	0.20	0	0.13	0.65	0.17	0.45	0.82	0.79
Mo	0	0.04	0.04(B)	0.40	0.20	0.19	0.51	0.86
W	0	0.19	0.22	0.35	0.37	0.39	0.50	1.01
Mn	0.58	0	B	1.01	0.14	0.40	1.17	0.99
Fe	0.57	0	B	0.83	0.27	0.45	1.23	0.43
Co	0.87	0	0.30	0.81	0.26	0.44	1.49	0.22
Ni	1.42	0.57	0.15	1.45	0.76	1.17	1.91	0
Cu	1.43	0.49	0.67	1.34	0.73	1.03	1.83	0
Zn	0.92	0.34	0.42	1.03	0.54	0.91	1.53	0

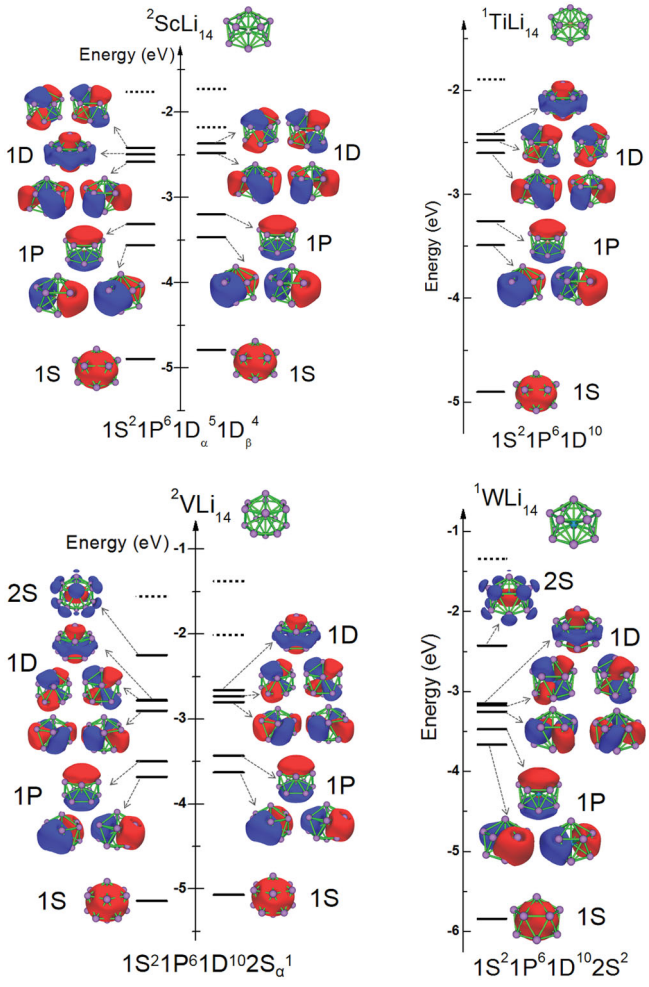

Figure 2. One electron energy levels and MOs of TM@Li_{14} (TM = Sc, Ti, V and W). Continuous lines correspond to the filled levels while the dotted lines correspond to the unfilled states. For each level, the degenerated energy states are arranged in a horizontal line. The surface isovalue for MO plotting is 0.022 e/Å^3.

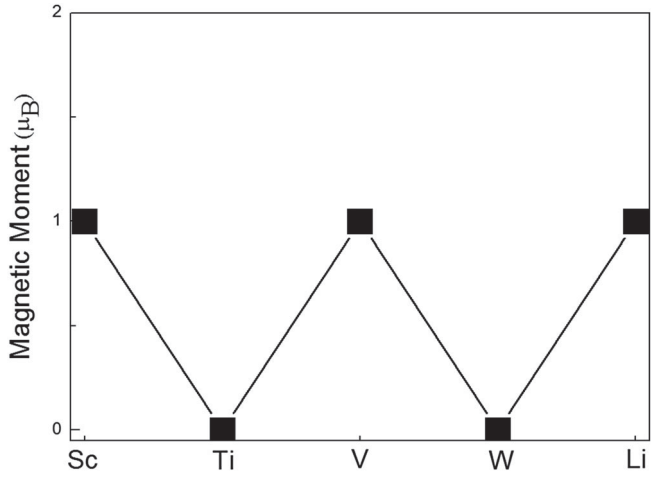

Figure 3. Diagram of the magnetic moment of TM@Li_{14} (TM = Sc, Ti, V and W) clusters and pure Li_{15} cluster.

the corresponding superatomic configuration of W@Li_{14} cluster is $1S^21P^61D^{10}2S^2$, with a closed electronic shell for the paired electrons occupation. According to the jellium model, the 20-electron W@Li_{14} cluster is very stable. Similar to this, the effective electronic configuration of titanium atom is $3d^24s^2$, and the corresponding filling order of Ti@Li_{14} cluster is $1S^21P^61D^{10}$, of which the MO diagrams are also shown in Figure 2. On account of the full electrons of S, P, D super-MOs, W@Li_{14} cluster and Ti@Li_{14} cluster are both nonmagnetic and the total valence electrons fulfil the 20-electron rule and the 18-electron rule, respectively.

For V@Li_{14} cluster, the number of total effective valence electrons is 19 based on the above analysis. Both the one-electron energy levels and MOs are displayed in Figure 2. Following this picture, the filling of both spin states corresponds to a $1S^21P^61D^{10}2S_\alpha{}^1$ superatomic configuration with one unpaired $2S_\alpha$ electron, which makes V@Li_{14} cluster with a magnetic moment of 1 μ_B. Analogously, the total effective electrons are 17 for the Sc@Li_{14} cluster, forming a $1S^21P^61D_\alpha{}^51D_\beta{}^4$ electronic configuration. Also, the Sc@Li_{14} cluster is a magnetic superatom with a low spin magnetic moment of 1.0 μ_B.

These features indicate that a transition-metal atom embedded into Li_{14} cage tends to form superatoms, of which the stability is effected by the electronic and geometric shells [44,45]. On the basis of the jellium model, the stability of TM@Li_{14} (TM = Ti and W) is enhanced by their closed electronic and geometric shells, filling the 18-electron rule and 20-electron rule, respectively. For TM@Li_{14} (TM = Sc and V), both with a partially filled subshell, they can stabilise themselves via spin multiplicities. Correspondingly, the total effective valence electrons are between 17 and 20, and the total magnetic moment is changing between 0 with 1 μ_B for TM@Li_{14} (TM = Sc, Ti, V and W) clusters, exhibiting a remarkable odd-even alternation, as shown in Figure 3. The findings are developing with binary lithium superatoms compared with the previous researches of VLi_n (n = 1–13) clusters reported by Zhang et al. [29] and of M@Li_{16} (M = Ca, Sr, Ba, Ti, Zr, Hf) reported by Gu et al. [14]. However, not all the transition-metal doped TM@Li_{14} clusters are suitable for the D_{6d} symmetry superatomic structures due to the number of valence electrons and the mismatch of atomic radius. That's why the lowest energy structures of TM@Li_{14} clusters using Cr, Mo and W atoms as dopants, which have the same effective valence electrons, are diverse as shown in Table 1.

To further discuss the stability of TM@Li_{14} (M = Sc, Ti, V and W) clusters with the D_{6d} symmetry lowest-energy structures, we calculate the average binding energy (E_b) per atom and the fragmentation energy (E_f),

Table 2. The results of calculated Symmetry, Fragmentation Energy (E_f), Average Binding Energy (E_b) Per Atom, Embedding Energy (D_e), HOMO–LUMO Gaps (E_{gap}) and Total Magnetic Moment (μ_s) of TM@Li_{14} (TM = Sc, Ti, V and W) and that of the corresponding pure Li_{15} cluster by Gaussian 16.

TM	Methods	Symm.	E_f (eV)	E_b (eV)	D_e (eV)	E_{gap} (eV)	μ_s (μ_B)
Sc	PW91	D_{6d}	1.94	1.27	3.97	0.50	1
	M06L		2.03	1.37	4.26	0.12	
	TPSSH		1.93	1.24	3.60	0.64	
Ti	PW91	D_{6d}	1.62	1.42	6.25	0.39	0
	M06L		1.80	1.49	6.11	0.39	
	TPSSH		1.65	1.36	5.39	0.81	
V	PW91	D_{6d}	1.35	1.32	4.80	0.22	1
	M06L		1.40	1.40	4.72	0.13	
	TPSSH		1.45	1.38	5.68	0.63	
W	PW91	D_{6d}	1.36	1.69	10.33	0.99	0
	M06L		1.43	1.69	9.10	0.93	
	TPSSH		1.27	1.60	8.93	1.35	
Li_{15}	PW91	C_{2v}	1.30	1.09	–	0.28	1
	M06L		1.35	1.18	–	0.30	
	TPSSH		1.29	1.09	–	0.78	

which are respectively defined as:

$$E_b(TM@Li_{14}) = [E(TM) + 14E(Li) - E(TM@Li_{14})]/15$$

$$E_f(TM@Li_{14}) = E(TM@Li_{13}) + E(Li) - E(TM@Li_{14})$$

Where TM represents the transition-metal Sc, Ti, V and W atoms. E(TM@Li_{14}) and E(TM@Li_{13}) represent the total energy of the lowest-energy structures of TM@Li_{14} clusters and TM@Li_{13} cluster, respectively. E(Li) and E(TM) are the total energy of the Li atom and transition-metal atoms in the free state, respectively. In addition, the embedding energy (D_e) between an embedded atom with the embedded shell of TM@Li_{14} (M = Sc, Ti, V and W) clusters are also calculated using the following equation:

$$D_e(TM@Li_{14}) = E(shell) + E(core) - E(TM@Li_{14})$$

In the above equation, E(shell), E(core) and E(TM@Li_{14}) are the energies of cages, transition-metal atoms and TM@Li_{14} clusters, respectively. Correspondingly, the positive D_e values indicate that these transition-metal atoms can be embedded into the Li_{14} cage. Table 2 gives the calculated energies, which are drawn in Figure 4 for clarity. From the results of the average binding energies per atom, it can be noticed that all the lowest-energy structures of TM@Li_{14} (TM = Sc, Ti, V and W) clusters, which are cage-like structures with the centre encapsulated by a transition-metal atom (high D_{6d} symmetry), are stable. With the increasing electron counts, the fragmentation energies of TM@Li_{14} (TM = Sc, Ti, V and W) is decreasing in succession, and thus to dissociate easier. From the view of coordination compounds, the trend can well understand because a core atom only could handle a certain number of coordinations. For transition-metal atom doped lithium superatom systems, 20-electron is

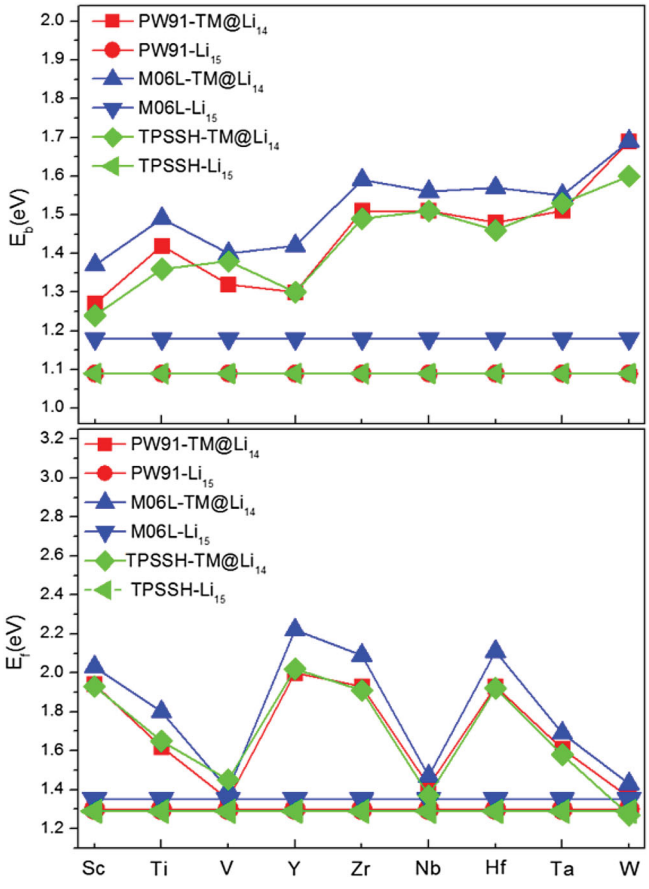

Figure 4. The average binding energies per atom (E_b) and fragmentation energies (E_f) of TM@Li_{14} (TM = Sc, Ti, V, Y, Zr, Nb, Hf, Ta and W) clusters and pure Li_{15} cluster for the lowest-energy structures.

the maximum value [14]. So the D_{6d} symmetry systems are not the lowest energy isomer while other transition-metal atoms as dopants. The positive D_e values prove the feasibilities of doping transition-metal atoms into Li_{14}

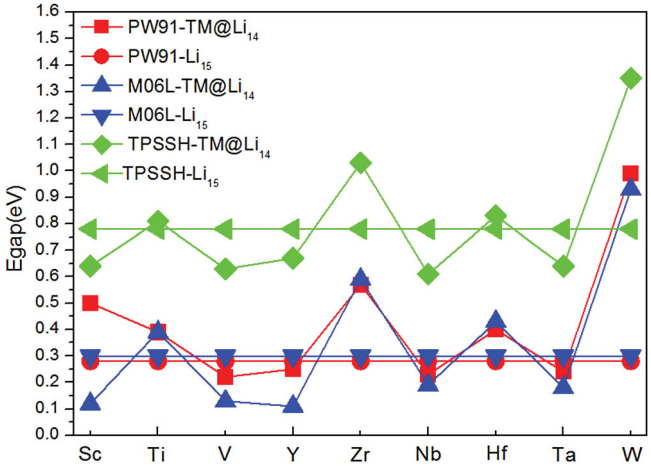

Figure 5. Comparison of the HOMO–LUMO energy gap (E_{gap}) of $TM@Li_{14}$ (TM = Sc, Ti, V, Y, Zr, Nb, Hf, Ta and W) clusters and pure Li_{15} cluster for the lowest-energy structures.

cage. The large D_e value of $W@Li_{14}$ cluster indicates that the tungsten atom is more preferable as a dopant.

The energy gap (E_{gap}) is now known another quantity that can examine energetic stability of small clusters, which is the energy differences between the highest occupied molecular orbital (HOMO) and the lowest unoccupied molecular orbital (LUMO). The HOMO–LUMO gaps for all the lowest energy structures $TM@Li_{14}$ (TM = Sc, Ti, V, and W) are shown in Table 2 and Figure 5. Especially, 20-electron $W@Li_{14}$ cluster is with a particularly large E_{gap} 0.99 eV at GGA/PW91/SDD level, which further enhances its stability. A more accurate gap of $W@Li_{14}$ cluster is 1.35 eV given by hybrid functionals TPSSH/SDD for that the standard GGA functionals often underestimate the gaps. Moreover, the gaps of 18-electron systems and 20-electron systems are apparently larger than that of the clusters with nearest effective valence electrons. This predicts their high stability.

Summary and conclusions

To summarise, combining CALYPSO structure prediction method with density-functional theory calculations, we have shown that the replacement a lithium atom in the bare Li_{15} cluster with a transition-metal atom (TM = Sc, Ti, V, Y, Zr, Nb, Hf, Ta and W) can give rise to D_{6d} symmetry cage-like $TM@Li_{14}$ clusters, where the transition-metal atom is located in the centre of the cage. The stability of D_{6d} symmetry $TM@Li_{14}$ (TM = Sc, Ti, V and W) clusters can be explained well based on the superatoms or magnetic superatoms model. Among them, $W@Li_{14}$ cluster and $Ti@Li_{14}$ cluster are nonmagnetic superatoms, for all of their effective valence electrons are paired fulfilling the 20-electron rule and 18-electron rule, respectively. $Sc@Li_{14}$ cluster and $V@Li_{14}$ cluster are identified as magnetic superatoms, both of them with a magnetic moment of 1 μ_B. Moreover, with the variation of doped transition-metal elements, the total magnetic moment of $TM@Li_{14}$ (TM = Sc, Ti, V and W) clusters exhibit a remarkable odd-even alternation (between 0 with 1 μ_B, respectively). These properties of $TM@Li_{14}$ (TM = Sc, Ti, V and W) series can be expanded to the elements in the same main group as the dopants due to with the same effective valance electrons to Sc, Ti and V atoms, respectively. Comparing with the original Li_{15} cluster, the stability and the properties of $TM@Li_{14}$ (TM = Sc, Ti, V, Y, Zr, Nb, Hf, Ta and W) clusters have changed dramatically by fusing transition-metal elements with lithium atoms, which is a feasible route to synthesise superatoms with specific features. These novel binary clusters are looking forward to serve as building blocks of nanoscale materials and devices in the future.

Disclosure statement

No potential conflict of interest was reported by the authors.

Funding

This work is supported by the National Natural Science Foundation of China [grant number 11704080], by the Special Foundation for theoretical physics Research Program of China [grant number 11847119], by the PhD Starting Fund of Guangdong Ocean University [grant numbers 120702/R17077 and 120702/R17055], by the Innovation and Strong School Research Project of Guangdong Ocean University [grant number GDOU2017052621], and Shenzhen Supercomputer Centers.

References

[1] S.N. Khanna and P. Jena, Phys. Rev. **B 51**, 13705 (1995).
[2] S.A. Claridge, J.A.W. Castleman, S.N. Khanna, C.B. Murray, A. Sen and P.S. Weiss, ACS Nano. **2**, 244 (2009).
[3] P. Jena and Q. Sun, Chem. Rev. **118**, 5755 (2018).
[4] A. Pinkard, A.M. Champsaur and X. Roy, Acc. Chem. Res. **51**, 919 (2018).
[5] J.A.W. Castleman and S.N. Khanna, J. Phys Chem. C. **113**, 2664 (2009).
[6] W.D. Knight, K. Clemenger, W.A. de Heer, W.A. Saunders, M.Y. Chou and M.L. Cohen, Phys. Rev. Lett. **52**, 2141 (1984).
[7] D.E. Bergeron, A.W.C. Castleman Jr., T. Morisato and S.N. Khanna, Science **304**, 84 (2004).
[8] W. Ekardt, Phys. Rev. B. **29**, 1558 (1984).
[9] W. Ekardt, Phys. Rev. B. **34**, 526 (1986).
[10] M. Brack, Rev. Mod. Phys. **65**, 677 (1993).
[11] J.U. Reveles, P.A. Clayborne, A.C. Reber, S.N. Khanna, K. Pradhan, P. Sen and M.R. Pederson, Nat. Chem. **1**, 310 (2009).

[12] H. He, R. Pandey, J.U. Reveles, S.N. Khanna and S.P. Karna, Appl. Phys. Lett. **95**, 192104 (2009).
[13] V. Chauhan, V.M. Medel, J. Ulises Reveles, S.N. Khanna and P. Sen, Chem. Phys. Lett. **528**, 39 (2012).
[14] X. Gu, G.H. Chen, M. Ji, Y.X. Yao and X.G. Gong, Nanoscale **4**, 2567 (2012).
[15] V. Medel, J.U. Reveles and S.N. Khanna, J. Appl. Phys. **112**, 064313 (2012).
[16] X. Zhang, Y. Wang, H. Wang, A. Lim, G. Gantefoer, K.H. Bowen, J.U. Reveles and S.N. Khanna, J. Am. Chem. Soc. **135**, 4856 (2013).
[17] V.M. Medel, A.C. Reber, V. Chauhan, P. Sen, A.M. Koster, P. Calaminici and S.N. Khanna, J. Am. Chem. Soc. **136**, 8229 (2014).
[18] A. Lebon, A. Aguado and A. Vega, Phys. Chem. Chem. Phys. **17**, 28033 (2015).
[19] V. Etacheri, R. Marom, R. Elazari, G. Salitra and D. Aurbach, Energy Environ. Sci. **4**, 3243 (2011).
[20] W.-J. Zhang, J. Power Sources. **196**, 13 (2011).
[21] H. S. i. M. M.-O. Frameworks, Science. **300**, 1127 (2003).
[22] L.J. Murray, M. Dinca and J.R. Long, Chem. Soc. Rev. **38**, 1294 (2009).
[23] L.J. Cheng and J.L. Yang, J. Chem. Phys. **138**, 141101 (2013).
[24] L. Cheng, X. Zhang, B. Jin and J. Yang, Nanoscale **6**, 12440 (2014).
[25] L.J. Yan, L.J. Cheng and J.L. Yang, J. Phys. Chem. C. **119**, 23274 (2015).
[26] L.J. Yan, L.J. Cheng and J.L. Yang, Chin. J. Chem. Phys. **28**, 476 (2015).
[27] H. Wang and L. Cheng, Nanoscale **9**, 13209 (2017).
[28] R. Fournier, J. Bo Yi Cheng and A. Wong, J. Chem. Phys. **119**, 9444 (2003).
[29] M. Zhang, J. Zhang, X. Feng, H. Zhang, L. Zhao, Y. Luo and W. Cao, J. Phys. Chem. A. **117**, 13025 (2013).
[30] P. Guo, L. Fu, J. Zheng, P. Zhao, Y. Wan and Z. Jiang, Appl. Surf. Sci. **465**, 207 (2019).
[31] J. Lv, Y. Wang, L. Zhu and Y. Ma, J. Chem. Phys. **137**, 084104 (2012).
[32] J.P. Perdew and Y. Wang, Phys. Rev. B. **45**, 13244 (1992).
[33] J.P. Perdew, K. Burke and M. Ernzerhof, Phys. Rev. Lett. **77**, 3865 (1996).
[34] N. Mardirossian and M. Head-Gordon, Mol. Phys. **115**, 2315 (2017).
[35] L. Goerigk, A. Hansen, C. Bauer, S. Ehrlich, A. Najibi and S. Grimme, Phys. Chem. Chem. Phys. **19**, 32184 (2017).
[36] T. Weymuth, E.P.A. Couzijn, P. Chen, M. Reiher and J. Chem, Theory Comput. **10**, 3092 (2014).
[37] S. Dohm, A. Hansen, M. Steinmetz, S. Grimme, M.P. Checinski and J. Chem, Theory Comput. **14**, 2596 (2018).
[38] Y. Zhao and D.G. Truhlar, J. Chem. Phys. **125**, 194101 (2006).
[39] V. Staroverov, G. Scuseria, J. Tao and J. Perdew, J. Chem. Phys. **119**, 12129 (2003).
[40] D.Y. Zubarev and A.I. Boldyrev, Phys. Chem. Chem. Phys. **10**, 5207 (2008).
[41] P.J. Hay and W.R. Wadt, J. Chem. Phys. **82**, 270 (1985).
[42] M. J. Frischet al., *Gaussian 16, Revision B.01* (Gaussian Inc., Wallingford, CT, 2016).
[43] T. Lu and F. Chen, J. Comput. Chem. **33**, 580 (2012).
[44] A.C. Reber and S.N. Khanna, Acc. Chem. Res. **50**, 255 (2017).
[45] Z. Luo and A.W. Castleman, Acc. Chem. Res. **47**, 2931 (2014).